Multi-Agent Safe Policy Learning for Power Management of Networked Microgrids

Qianzhi Zhang, *Student Member, IEEE,* Kaveh Dehghanpour, *Member, IEEE,* Zhaoyu Wang, *Member, IEEE,* Feng Qiu, *Senior Member, IEEE,* and Dongbo Zhao, *Senior Member, IEEE*

arXiv:1907.02091v2 [eess.SY] 18 Oct 2019

***Abstract*—This paper presents a multi-agent safe policy learning (PL) method for optimal power management of networked microgrids (MGs) in distribution systems. While conventional reinforcement learning (RL) algorithms are *black box* decision models that could fail to satisfy grid operational constraints, our proposed method is constrained by AC power flow equations and other operational limits. Accordingly, the training process employs the gradient information of operational constraints to ensure that the optimal control policy functions generate safe and feasible decisions. Furthermore, we have proposed a multi-agent primal-dual consensus-based training approach for the PL solver to maintain the privacy of MGs' control policies in a distributed way. After training, the learned optimal policy functions can be safely used by the MGs to dispatch their local resources, without the need to solve a complex optimization problem from scratch. Numerical experiments have been devised to verify the performance of the proposed method.**

***Index Terms*—Safe policy learning, multi-agent framework, networked microgrids, power management, policy gradient.**

I. Introduction

NETWORKED microgrids (MGs) can offer various benefits, including higher perpetration of local distributed energy resources (DERs), improved controllability, and enhancement of power system resilience and reliability [1], [2]. Solving the power management problem of networked MGs is a complex task. While previous works in this area have provided valuable insight, we have identified two shortcomings in the literature:

(1) *Limitations of model-based optimization methods:* In the existing literature, there are quite a few model-based methods for solving the optimal power management problem of networked MGs, such as centralized decision models [3], [4] and distributed control frameworks [5]–[7]. However, with increasing number of MGs in distribution networks, these methods have to solve large-scale optimization problems with numerous nonlinear constraints that incur high computational costs and hinder real-time decision making. Furthermore, model-based methods are unable to adapt to the continuously evolving system conditions, as they need to re-solve the problem at each time step.

(2) *Potential infeasibility of model-free machine learning methods:* To address the limitations of model-based methods, model-free reinforcement learning (RL) techniques have been used to solve the optimal power management problem through repeated interactions between a control agent and its environment. This approach eliminates the need to solve a large-scale optimization problem at each time point and enables the control agent to provide adaptive response to time-varying system states. Existing examples of RL application in power systems include economic dispatch and energy consumption scheduling of individual MGs [8]–[10] and multi-area smart control of generation in interconnected power grids [11], [12]. In our previous paper [12], we proposed a bi-level power management method for networked MGs, where a centralized RL agent determines retail prices in a cooperative business model for each MG under the incomplete information of physical model. Current RL-based solutions employ control agents to train *black box* functions to approximate the optimal actions through trial and error. However, the trained black box functions can fail to satisfy critical operational constraints, such as nodal voltage and capacity limits, since these constraints have not been encoded in the training process. This can lead to unsafe operational states and control action infeasibility.

Inspired by recent advances in constrained policy learning (PL) [13]–[15] and to address the shortcomings in the existing literature, we have cast the power management of networked MGs as a *safe PL problem*. Moreover, we have proposed a multi-agent policy gradient solution strategy to learn optimal control policies for the networked MGs in a distributed way. The proposed method introduces a trade-off between model-free and model-based methods and combines the benefits offered by both sides. Hence, on one hand, MGs' power management policy functions are modeled using black box deep neural networks (DNNs); while on the other hand, to ensure decision feasibility, a constrained back-propagation training method is proposed that exploits the gradients of the constraints and objective functions of the power management problem. The training process employs these gradient factors to provide a convex quadratically constrained linear program (QCLP) approximation to the power management problem at each back-propagation iteration. This enables the proposed method to be both adaptable to changes in the inputs of the black box components, and feasible with respect to operational constraints, including AC power flow. Finally, a distributed consensus-based primal-dual optimization method is proposed to decompose the training task among MG agents [16]. The distributed computation offers two advantages: (i) maintaining the privacy of MG control policies, and (ii) enhancing compu-

Q. Zhang, K. Dehghanpour, and Z. Wang are with the Department of Electrical and Computer Engineering, Iowa State University, Ames, IA 50011 USA (e-mail: wzy@iastate.edu).

F. Qiu and D. Zhao are with Energy Systems Division, Argonne National Laboratory, Lemont, IL 60439 USA (e-mail: fqiu@anl.gov, dongbo.zhao@anl.gov).

tational efficiency as the number of learning parameters grow. Furthermore, compared to existing work including ours, the main advances of this paper are as follows: (1) while [12] was based on a complex centralized solver, here we have proposed a distributed framework with multi-agent to perform safe PL without a central agent; (2) while previous work falls under the category of model-free RL, which can potentially generate infeasible control actions. However, incorporating constraints into the training process of conventional black box methods is challenging since these methods have generally relied on adding penalty terms to training objective functions for enforcing constraints, which cannot guarantee the safety of control policies as the number of constraints grows. Our idea is to leverage the gradient information of all the operational constraints to devise a tractable QCLP-based training process to guarantee the safety and feasibility of control policies.

The reminder of the paper is organized as follows: Section II presents the overall framework of the proposed solution. Section III introduces the safe PL problem and integrates problem gradients into the solver. Section IV describes the multi-agent consensus-based algorithm for safe PL. Simulation results and conclusions are given in Section V and Section VI, respectively.

II. Overview of the Proposed Framework

The general framework of the proposed multi-agent safe PL method is shown in Fig. 1. Note that vectors are denoted in bold letters throughout the paper. The micro-sources within each MG are controlled by an agent that adopts a private control policy. Here, the *control policy* for the n'th agent, , π_n, is a parametric probability distribution function, with parameters $\boldsymbol{\theta_n}$, over the agent's control actions ($\boldsymbol{a_n(t)}$), including active/reactive power dispatching signals for local diesel generators (DGs), energy storage system (ESS) and solar photo-voltaic (PV) panels. Note that the control policy π_n is a function of the MG's state variables ($\boldsymbol{S_n(t)}$), defined by the aggregate MG load and solar irradiance. To ensure the safety of the control policies, MG agents receive the observed variables from the grid, including network nodal voltages $\boldsymbol{V(t)}$ and injection currents $\boldsymbol{I(t)}$, to determine gradient factors of the problem constraints and objectives w.r.t. to learning parameters, $\nabla_{\boldsymbol{\theta}}\boldsymbol{J}$. These gradient factors are then integrated into a multi-agent constrained back-propagation algorithm, which employs local inter-MG communication to satisfy all global and local operational constraints through exchanging and processing dual Lagrangian variables, λ(t). Theoretical analysis and numerical simulations are conducted to show that the proposed safe PL method can maximize the MG agents' payoffs and satisfy operational constraints.

III. Safe Policy Learning for Power Management of Networked MGs

To facilitate the discussion, Section III-A introduces a general power management formulation that is commonly used in literature [4], [5], [12]. In Sections III-B and III-C, we propose a new tractable safe PL method, employing the problem's gradient factors, to solve the power management of networked MGs.

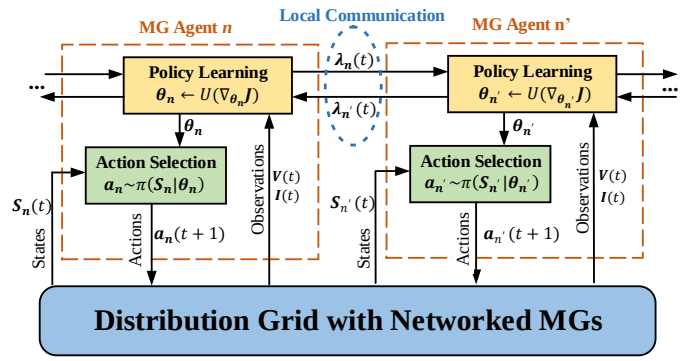

Fig. 1. Structure of the proposed multi-agent safe PL method for power management of networked MGs

A. Power Management Problem Statement

Each MG is assumed to have local DGs, ESS, solar PV panels and a number of loads. This optimization problem is solved over a moving look-ahead decision window $t' \in [t, t+T]$, using the latest estimations of solar and load power at different instants. Here, n is the MG index ($n \in \{1, ..., N\}$), i and j define the node numbers ($\forall i, j \in \Omega_i$), and l denotes the network branch index ($\forall l \in \Omega_L$).

*1) **Problem objective***: The objective function (1), with control action vector $[P^{DG}, P^{Ch}, P^{Dis}, Q^{DG}, Q^{PV}, Q^{ESS}] \in (\boldsymbol{x_p}, \boldsymbol{x_q})$, minimizes MGs' total cost of operation, which is composed of the income/cost from power transfer with the grid and cost of running local DG. Here, λ_n^F is the DG fuel price in $\$/L$, $\lambda_{n,t'}^R$ is the electricity price in $\$/kWh$, and $P_{n,t'}^{PCC}$ is active power transfer between grid and the n'th MG at the point of common coupling (PCC). The fuel consumption of DG, $F_{i,n,t'}$, can be expressed as a quadratic polynomial function of its power, $P_{i,n,t'}^{DG}$, with parameters, a_n^f, b_n^f, and c_n^f, as shown in (2).

$$\min_{\boldsymbol{x_p}, \boldsymbol{x_q}} \sum_{n=1}^{N} \sum_{t'=t}^{t+T} (-\lambda_{n,t'}^R P_{n,t'}^{PCC} + \lambda_{i,n,t'}^F F_{i,n,t'}) \tag{1}$$

$$F_{i,n,t'} = a_n^f (P_{i,n,t'}^{DG})^2 + b_n^f P_{i,n,t'}^{DG} + c_n^f \tag{2}$$

*2) **Global constraints***: These constraints are defined over variables that are impacted by control actions of all the MGs, including the voltage amplitude limits for the entire nodes, $[V_i^m, V_i^M]$, and the maximum permissible branch current flow magnitudes I_{ij}^M throughout the distribution grid and the MGs:

$$V_i^m \leq V_{i,t'} \leq V_i^M \tag{3}$$

$$-I_{ij}^M \leq I_{ij,t'} \leq I_{ij}^M \tag{4}$$

Note that the global constraints are implicitly determined by the AC power flow equations, which will be used to calculate the gradient factors of objective (1) and constraints (3)-(14) w.r.t. learning parameters as elaborated in Section III-C.

*3) **Local constraints***: These constraints are defined over the local control actions of each MG. Constraints (5)-(6) ensure that the DG active/reactive power outputs, $P_{i,n}^{DG}/Q_{i,n}^{DG}$, are within the DG power capacity $P_{i,n}^{DG,M}/Q_{i,n}^{DG,M}$, and (7) enforces the maximum DG ramp limit, $P_{i,n}^{DG,R}$. PV reactive

power output, $Q_{i,n}^{PV}$, is constrained by its maximum limit $Q_{i,n}^{PV,M}$ per (8).

$$0 \leq P_{i,n,t'}^{DG} \leq P_{i,n}^{DG,M} \tag{5}$$

$$0 \leq Q_{i,n,t'}^{DG} \leq Q_{i,n}^{DG,M} \tag{6}$$

$$|P_{i,n,t'}^{DG} - P_{i,n,t'-1}^{DG}| \leq P_{i,n}^{DG,R} \tag{7}$$

$$|Q_{i,n,t'}^{PV}| \leq Q_{i,n}^{PV,M} \tag{8}$$

The operational ESS constraints are described by (9)-(14), where (9) determines the state of charge (SOC) of ESSs, $SOC_{i,n}$. $E_{i,n}^{Cap}$ denotes the maximum capacity of ESSs. To ensure safe ESS operation, the SOC and charging/discharging power of ESS, $P_{i,n}^{Ch}$, $P_{i,n}^{Dis}$, are constrained as shown in (10)-(14). Here, $[SOC_{i,n}^{m}, SOC_{i,n}^{M}]$, $P_{i,n}^{Ch,M}$ and $P_{i,n}^{Dis,M}$ define the permissible range of SOC, and maximum charging and discharging power, respectively. Constraint (13) indicates that ESSs cannot charge and discharge at the same time instant. And η_{Ch}/η_{Dis} represents the charging/discharging efficiency. The reactive power of ESS, $Q_{i,n}^{ESS}$, is kept within maximum limit, $Q_{i,n}^{ESS,M}$, through constraint (14).

$$SOC_{i,n,t'} = SOC_{i,n,t'-1} + \Delta t \frac{(P_{i,n,t'}^{Ch}\eta_{Ch} - P_{i,n,t'}^{Dis}/\eta_{Dis})}{E_{i,n}^{Cap}} \tag{9}$$

$$SOC_{i,n}^{m} \leq SOC_{i,n,t'} \leq SOC_{i,n}^{M} \tag{10}$$

$$0 \leq P_{i,n,t'}^{Ch} \leq P_{i,n}^{Ch,M} \tag{11}$$

$$0 \leq P_{i,n,t'}^{Dis} \leq P_{i,n}^{Dis,M} \tag{12}$$

$$P_{i,n,t'}^{Ch} P_{i,n,t'}^{Dis} = 0 \tag{13}$$

$$|Q_{i,n,t'}^{ESS}| \leq Q_{i,n}^{ESS,M} \tag{14}$$

B. Proposed Safe Policy Learning Formulation

Our solution consists of multiple autonomous MG agents, where each agent is in charge of dispatching the resources within an individual MG. The MGs are *collaborative*, in the sense that they depend on local communication with each other to optimize their behaviors. We propose transforming the power management problem of the networked MGs (1)-(14) into an iterative safe PL problem, where the control policies of the agents are updated at time t, around their latest values, by maximizing a reward function while satisfying constraint return criteria:

$$\boldsymbol{\pi}^{t+1} = \underset{\pi_1,...,\pi_N}{\arg\max} \sum_{n=1}^{N} J_{R_n}(\pi_n) \tag{15}$$

$$s.t. \;\; \boldsymbol{a_n} \sim \pi_n(\boldsymbol{S_n}) \tag{16}$$

$$J_{C_m}(\boldsymbol{\pi}) \leq d_m, \; \forall m \tag{17}$$

$$\Delta(\pi_n, \pi_n^t) \leq \delta, \; \forall n \tag{18}$$

where, $\boldsymbol{\pi} = [\pi_1, ..., \pi_n]$ denotes the set of control policies of all agents, with π_n defined as a multivariate distribution function over the agent's control actions $\boldsymbol{a_n} \in \mathbb{R}^{D_n}$, consisting of the dispatching decision variables. Note that, as seen in (16), the agent's policy is a function of the state vector $\boldsymbol{S_{n,t}}$, which consists of the estimated solar irradiance and aggregate internal load power of the n'th MG within the decision time window, $[t, t+T]$. The reward function for the n'th MG, $J_{R_n}(\pi_n)$, is defined as the negative accumulated operational cost of networked MGs over the decision window, obtained from the objective function of the power management problem, (1), as follows: .

$$J_{R_n}(\pi_n) = E_{\pi_n}[\sum_{t'=t}^{t+T}(\lambda_{n,t'}^{R} P_{n,t'}^{PCC} - \lambda_{i,n,t'}^{F} F_{i,n,t'})] \tag{19}$$

where, $E_{\pi_n}\{\}$ is the expectation operation over the control policy of the agent, to take the inherent uncertainty of the problem into account. Furthermore, in (17), the expected return values $J_{C_m}(\boldsymbol{\pi}) = E_{\boldsymbol{\pi}}(C_m)$ are used to ensure the satisfaction of m'th constraint, $C_m \leq d_m$, based on the control policies. The problem consists of a total of M constraints, including M^L local and M^G global constraints, defined by (3)-(4) and (5)-(14), respectively. Note that equality constraints (13) can be transformed into two inequality constraints. In (18), $\Delta(\cdot,\cdot)$ is the KL-divergence function [13] that serves as a distance measure between the previous policy, π_n^t, and the updated policy, π_n^{t+1}, and is constrained by a step size, δ. Note that (18) ensures that consecutive policies are within close distance from each other.

As shown in [13], the intractable non-convex PL formulation (15)-(18) can be transformed into a tractable convex iterative QCLP. To do this, the control policies of MG agents need to be parameterized in the first place. We propose a general and flexible parameterization scheme, in which two DNNs are employed for each MG agent to represent the control actions mean vector, $\boldsymbol{\mu_n} \in \mathbb{R}^{D_n \times 1}$, and covariance matrix $\Sigma_n \in \mathbb{R}^{D_n \times D_n}$. Hence, the DNNs receive the local states as input to fully quantify the mean vector and the covariance matrix of the agent's control actions, as follows:

$$\boldsymbol{\mu}_n = DNN(\boldsymbol{S_n}|\boldsymbol{\theta_{\mu_n}}) \tag{20}$$

$$\Sigma_n = DNN(\boldsymbol{S_n}|\boldsymbol{\theta_{\Sigma_n}}) \tag{21}$$

where, the agent's learning parameter vector, $\boldsymbol{\theta_n}$, consists of two parametric subsets $\boldsymbol{\theta_{\mu_n}}$ and $\boldsymbol{\theta_{\Sigma_n}}$. Thus, $\boldsymbol{\theta_{\mu_n}}$ and $\boldsymbol{\theta_{\Sigma_n}}$ are basically the weights and biases of the agent's DNNs. Then, the agents' control policies can be determined by embedding the parameterized learning structures (20) and (21) into D_n-dimensional multivariate Gaussian distribution functions over control actions $\boldsymbol{a_n}$ as follows:

$$\boldsymbol{a_n} \sim \pi_n(\boldsymbol{S_n}|\boldsymbol{\theta_n}) = \frac{1}{\sqrt{|\Sigma_n|(2\pi)^{D_n}}} e^{-\frac{1}{2}(\boldsymbol{a_n}-\boldsymbol{\mu_n})^\top \Sigma_n^{-1}(\boldsymbol{a_n}-\boldsymbol{\mu_n})} \tag{22}$$

The QCLP enables learning the PL parameters, $\boldsymbol{\theta} = \{\boldsymbol{\theta_1}, ...\boldsymbol{\theta_N}\}$, using a trust region method [13], which is based on linear approximations of the objective and constraint returns around the latest parameter values, $\boldsymbol{\theta}^t$:

$$\boldsymbol{\theta^{t+1}} = \underset{\boldsymbol{\theta_1},...,\boldsymbol{\theta_N}}{\arg\max} \sum_{n=1}^{N} \boldsymbol{g_n}^T(\boldsymbol{\theta_n} - \boldsymbol{\theta_n^t}) \tag{23}$$

$$s.t. \;\; J_{c_m}(\boldsymbol{\theta^t}) + \boldsymbol{b_m}^T(\boldsymbol{\theta} - \boldsymbol{\theta^t}) \leq d_m, \; \forall m \tag{24}$$

$$\frac{1}{2}(\boldsymbol{\theta_n} - \boldsymbol{\theta_n^t})^T H_n(\boldsymbol{\theta_n} - \boldsymbol{\theta_n^t}) \leq \delta, \ \forall n \tag{25}$$

where, $\boldsymbol{g_n} = \nabla_\theta J_R$ and $\boldsymbol{b_m} = \nabla_\theta J_{C_m}$ are the *gradient factors* of the reward and constraint return functions w.r.t. the learning parameters. Constraint (18) is transformed into (25) using the Fisher information matrix (FIM) of the policy functions, π_n, denoted by H_n. The FIM is a positive semi-definite matrix, whose (c, d)'th entry for policy functions with a Gaussian structure is determined as follows [17]:

$$\begin{aligned} H_n(c,d) &= \varepsilon\left(\frac{\partial \log_p(X_n|\boldsymbol{\theta_n})}{\partial \boldsymbol{\theta_n}(c)} \frac{\partial \log_p(X|\boldsymbol{\theta_n})}{\partial \boldsymbol{\theta_n}(d)}\right) \\ &= 2\left(\frac{\partial \mu_n^H}{\partial \boldsymbol{\theta_n}(c)} \Sigma_n^{-1} \frac{\partial \boldsymbol{\mu_n}}{\partial \boldsymbol{\theta_n}(d)}\right) + \mathrm{Tr}\left\{\Sigma_n^{-1} \frac{\partial \Sigma_n}{\partial \boldsymbol{\theta_n}(c)} \Sigma_n^{-1} \frac{\partial \Sigma_n}{\partial \boldsymbol{\theta_n}(d)}\right\} \end{aligned} \tag{26}$$

Note that (23)-(25) provides a convexified constrained gradient-based method for training the policy functions of the MG agents. Thus, the gradient factors have to be determined for the two sets of learning parameters, $[\boldsymbol{\theta_{\mu_n}}, \boldsymbol{\theta_{\Sigma_n}}]$. This process is outlined in Section Section III-C.

C. Gradient Factor Determination

To determine gradient factors, the following information are used: (i) observations variables, $\boldsymbol{O_t}$, including grid's nodal voltages $\boldsymbol{V_t}$ and current injections $\boldsymbol{I_t}$, $\boldsymbol{O_t} = [\boldsymbol{V_t}, \boldsymbol{I_t}]$, provided by the nodal sensors or distribution grid's state estimation module. Note that the observations are implicitly determined by the agents' control actions, and thus, cannot be predicted independently of the agents' policies; (ii) the latest system states $\boldsymbol{S_n}$ for each MG agent. Unlike the observation variables, the state variables are independent of the agents' control actions and can be predicted for the whole decision window without the need to consider agents' policies; (iii) the latest control actions $\boldsymbol{a_n}$ of each MG agent; (iv) the latest learning parameters $\boldsymbol{\theta_n}$; (v) network parameters, including the nodal admittance matrix, Y. Using (i)-(v) and chain rule, $\boldsymbol{g_n}$ and $\boldsymbol{b_m}$ in (23) and (24) can be written as:

$$\boldsymbol{g_{\mu_n}} = \frac{\partial J_{R_n}}{\partial \boldsymbol{a_n}} \frac{\partial \boldsymbol{a_n}}{\partial \pi_n} \frac{\partial \pi_n}{\partial \boldsymbol{\mu_n}} \frac{\partial \boldsymbol{\mu_n}}{\partial \boldsymbol{\theta_{\mu_n}}}, \boldsymbol{b_{m,\mu_n}} = \frac{\partial J_{C_m}}{\partial \boldsymbol{a_n}} \frac{\partial \boldsymbol{a_n}}{\partial \pi_n} \frac{\partial \pi_n}{\partial \boldsymbol{\mu_n}} \frac{\partial \boldsymbol{\mu_n}}{\partial \boldsymbol{\theta_{\mu_n}}} \tag{27}$$

$$\boldsymbol{g_{\Sigma_n}} = \frac{\partial J_{R_n}}{\partial \boldsymbol{a_n}} \frac{\partial \boldsymbol{a_n}}{\partial \pi_n} \frac{\partial \pi_n}{\partial \Sigma_n} \frac{\partial \Sigma_n}{\partial \boldsymbol{\theta_{\Sigma_n}}}, \boldsymbol{b_{m,\Sigma_n}} = \frac{\partial J_{C_m}}{\partial \boldsymbol{a_n}} \frac{\partial \boldsymbol{a_n}}{\partial \pi_n} \frac{\partial \pi_n}{\partial \Sigma_n} \frac{\partial \Sigma_n}{\partial \boldsymbol{\theta_{\Sigma_n}}} \tag{28}$$

where, each gradient factor, $\boldsymbol{g_{\mu_n}}$, $\boldsymbol{b_{m,\mu_n}}$, $\boldsymbol{g_{\Sigma_n}}$, and $\boldsymbol{b_{m,\Sigma_n}}$, consists of four elements. All the elements in (27) and (28) can be obtained as follows:

1) $\partial J_{R_n}/\partial \boldsymbol{a_n}$ and $\partial J_{C_m}/\partial \boldsymbol{a_n}$: As can be seen in (5)-(14), the local constraint returns are trivial functions of the control actions. Hence, for these constraints, $\partial J_{C_m}/\partial \boldsymbol{a_n}$ can be directly calculated. For example, the constraint return value for (5) is $J_{C_{5,t'}} = P_{n,t'}^{DG}$ which induces a simple gradient element w.r.t. control action $P_{n,t'}^{DG}$:

$$\frac{\partial J_{C_{5,t'}}}{\partial P_{n,t'}^{DG}} = 1 \tag{29}$$

The gradients of returns w.r.t. control actions for the remaining constraints, (6)-(14), can be obtained in a similar way. The major difficulty in determining $\partial J_{R_n}/\partial \boldsymbol{a_n}$ and $\partial J_{C_m}/\partial \boldsymbol{a_n}$ pertains to the agents' reward functions and global constraint returns, (1)-(4), which are only implicitly related to the control actions. Since the reward and all the global constraint returns are functions of the observation variables, $\boldsymbol{V}$ and $\boldsymbol{I}$, the gradients of these variables w.r.t. control actions are obtained and used to quantify $\partial J_{R_n}/\partial \boldsymbol{a_n}$ and $\partial J_{C_m}/\partial \boldsymbol{a_n}$. To do this, a four-step process is proposed that leverages the current injection-based AC power flow equations:

TABLE I
DERIVATIONS OF $\boldsymbol{I^{Re}}$ AND $\boldsymbol{I^{Im}}$ W.R.T. $\boldsymbol{a_n}$

	$P_{n,t'}^{DG}$	$P_{n,t'}^{Ch}$	$P_{n,t'}^{Dis}$	$Q_{n,t'}^{DG}$	$Q_{n,t'}^{PV}$	$Q_{n,t'}^{ESS}$
$I_{i,t'}^{Re}$	$-\frac{V_{i,t'}^{Re}}{V_{i,t'}^2}$	$\frac{V_{i,t'}^{Re}}{V_{i,t'}^2}$	$-\frac{V_{i,t'}^{Re}}{V_{i,t'}^2}$	$\frac{V_{i,t'}^{Im}}{V_{i,t'}^2}$	$\frac{V_{i,t'}^{Im}}{V_{i,t'}^2}$	$-\frac{V_{i,t'}^{Im}}{V_{i,t'}^2}$
$I_{i,t'}^{Im}$	$-\frac{V_{i,t'}^{Im}}{V_{i,t'}^2}$	$\frac{V_{i,t'}^{Im}}{V_{i,t'}^2}$	$-\frac{V_{i,t'}^{Im}}{V_{i,t'}^2}$	$-\frac{V_{i,t'}^{Re}}{V_{i,t'}^2}$	$-\frac{V_{i,t'}^{Re}}{V_{i,t'}^2}$	$\frac{V_{i,t'}^{Re}}{V_{i,t'}^2}$

Step 1 - First, the gradients of real and imaginary parts of nodal current injection w.r.t. control actions are derived (denoted as $\partial \boldsymbol{I^{Re}}/\partial \boldsymbol{a_n}$ and $\partial \boldsymbol{I^{Im}}/\partial \boldsymbol{a_n}$, respectively.) To achieve this, the nodal power balance and nodal current injection relationships in the network are employed:

$$I_{i,t'}^{Re} = \frac{p_{i,n,t'} V_{i,t'}^{Re} + q_{i,n,t'} V_{i,t'}^{Im}}{V_{i,t'}^2} \tag{30}$$

$$I_{i,t'}^{Im} = \frac{p_{i,n,t'} V_{i,t'}^{Im} - q_{i,n,t'} V_{i,t'}^{Re}}{V_{i,t'}^2} \tag{31}$$

$$p_{i,n,t'} = P_{i,n,t'}^{D} - P_{i,n,t'}^{DG} - P_{i,n,t'}^{PV} + P_{i,n,t'}^{Ch} - P_{i,n,t'}^{Dis} \tag{32}$$

$$q_{i,n,t'} = Q_{i,n,t'}^{D} - Q_{i,n,t'}^{DG} - Q_{i,n,t'}^{PV} + Q_{i,n,t'}^{ESS} \tag{33}$$

where, I_i^{Re}, I_i^{Im} and V_i^{Re}, V_i^{Im} denote the real and imaginary parts of nodal voltage and current injection at node i. Using these equations, $\partial \boldsymbol{I^{Re}}/\partial \boldsymbol{a_n}$ and $\partial \boldsymbol{I^{Im}}/\partial \boldsymbol{a_n}$ are derived and shown in Table I. Note that the entries of this table can be calculated using the real and imaginary parts of nodal voltages, which in practice are either measured or estimated [18].

Step 2 - Using $\partial \boldsymbol{I^{Re}}/\partial \boldsymbol{a_n}$ and $\partial \boldsymbol{I^{Im}}/\partial \boldsymbol{a_n}$ from Step 1 (Table I), $\partial \boldsymbol{V^{Re}}/\partial \boldsymbol{a}$ and $\partial \boldsymbol{V^{Im}}/\partial \boldsymbol{a}$ are obtained employing the network-wide relationship between nodal voltages and current injections:

$$\begin{bmatrix} \frac{\partial \boldsymbol{V^{Re}}}{\partial \boldsymbol{a_n}} \\ \frac{\partial \boldsymbol{V^{Im}}}{\partial \boldsymbol{a_n}} \end{bmatrix} = \begin{bmatrix} Y^{11} & Y^{12} \\ Y^{21} & Y^{22} \end{bmatrix}^{-1} \begin{bmatrix} \frac{\partial \boldsymbol{I^{Re}}}{\partial \boldsymbol{a_n}} \\ \frac{\partial \boldsymbol{I^{Im}}}{\partial \boldsymbol{a_n}} \end{bmatrix} \tag{34}$$

where, the modified network bus admittance sub-matrices are determined as follows:

$$Y^{11} = Y^{Re} - Y_D^{(Re,Re)}, Y^{12} = -Y^{Im} - Y_D^{(Re,Im)} \tag{35}$$

$$Y^{21} = Y^{Im} - Y_D^{(Im,Re)}, Y^{22} = Y^{Re} - Y_D^{(Im,Im)} \tag{36}$$

here, Y^{Re} and Y^{Im} are the real and imaginary parts of the original bus admittance matrix. The elements in diagonal matrices $Y_D^{(Re,Re)}$, $Y_D^{(Re,Im)}$, $Y_D^{(Im,Re)}$ and $Y_D^{(Im,Im)}$ are calculated using the following equations [18]:

$$Y_D^{(Re,Re)}(i,i) = \frac{p_{i,n,t'}}{V_{i,t'}^2} - \frac{2V_{i,t'}^{Re}(p_{i,n,t'} V_{i,t'}^{Re} + q_{i,n,t'} V_{i,t'}^{Im})}{V_{i,t'}^4} \tag{37}$$

$$Y_D^{(Re,Im)}(i,i) = \frac{q_{i,n,t'}}{V_{i,t'}^2} - \frac{2V_{i,t'}^{Im}(p_{i,n,t'}V_{i,t'}^{Re} + q_{i,n,t'}V_{i,t'}^{Im})}{V_{i,t'}^4} \tag{38}$$

$$Y_D^{(Im,Re)}(i,i) = -\frac{q_{i,n,t'}}{V_{i,t'}^2} - \frac{2V_{i,t'}^{Re}(p_{i,n,t'}V_{i,t'}^{Im} - q_{i,n,t'}V_{i,t'}^{Re})}{V_{i,t'}^4} \tag{39}$$

$$Y_D^{(Im,Im)}(i,i) = \frac{p_{i,n,t'}}{V_{i,t'}^2} - \frac{2V_{i,t'}^{Im}(p_{i,n,t'}V_{i,t'}^{Im} - q_{i,n,t'}V_{i,t'}^{Re})}{V_{i,t'}^4} \tag{40}$$

Step 3 - Noting that the current flow constraint returns and the rewards are also functions of branch current flows, the gradients of branch current flows are required to obtain $\partial J_{R_n}/\partial \boldsymbol{a_n}$ and $\partial J_{C_m}/\partial \boldsymbol{a_n}$. Using the branch current flow equations, these gradients are determined as a function of the derivatives of nodal voltages and current injections, as follows:

$$\frac{\partial I_{ij,t'}^{Re}}{\partial \boldsymbol{a_{n,t'}}} = y_{ij}^{Im}(\frac{\partial V_{i,t'}^{Im}}{\partial \boldsymbol{a_{n,t'}}} - \frac{\partial V_{j,t'}^{Im}}{\partial \boldsymbol{a_{n,t'}}}) - y_{ij}^{Re}(\frac{\partial V_{i,t'}^{Re}}{\partial \boldsymbol{a_{n,t'}}} - \frac{\partial V_{j,t'}^{Re}}{\partial \boldsymbol{a_{n,t'}}}) \tag{41}$$

$$\frac{\partial I_{ij,t'}^{Im}}{\partial \boldsymbol{a_{n,t'}}} = y_{ij}^{Im}(\frac{\partial V_{i,t'}^{Re}}{\partial \boldsymbol{a_{n,t'}}} - \frac{\partial V_{j,t'}^{Re}}{\partial \boldsymbol{a_{n,t'}}}) + y_{ij}^{Re}(\frac{\partial V_{i,t'}^{Im}}{\partial \boldsymbol{a_{n,t'}}} - \frac{\partial V_{j,t'}^{Im}}{\partial \boldsymbol{a_{n,t'}}}) \tag{42}$$

where, I_{ij}^{Re} and I_{ij}^{Im} are the real and imaginary parts of branch currents, y_{ij}^{Re} and y_{ij}^{Im} are the real and imaginary parts of branch admittance.

Step 4 - Finally, using the derivatives obtained from Steps 1, 2, and 3, $\partial J_{R_n}/\partial \boldsymbol{a_n}$ and $\partial J_{C_m}/\partial \boldsymbol{a_n}$ are determined through straightforward algebraic manipulations. As an example, the gradient of reward function w.r.t. $P_{n,t'}^{DG}$ is calculated as:

$$\frac{\partial J_{R_n}}{\partial P_{n,t'}^{DG}} = \sum_{t'=t}^{t+T}(\lambda_{i,n,t'}^{F}(2a_f + b_f) - \lambda_{n,t'}^{R}\frac{\partial P_{n,t'}^{PCC}}{\partial P_{n,t'}^{DG}}) \tag{43}$$

where, $\partial P_{n,t'}^{PCC}/\partial P_{n,t'}^{DG}$ is obtained using the outcomes of Steps 2 and 3, as follows:

$$\frac{\partial P_{n,t'}^{PCC}}{\partial P_{n,t'}^{DG}} = \frac{\partial V_{i,t'}^{Re}}{\partial P_{n,t'}^{DG}} I_{ij,t'}^{Re} + V_{i,t'}^{Re}\frac{\partial I_{ij,t'}^{Re}}{\partial P_{n,t'}^{DG}} + \frac{\partial V_{i,t'}^{Im}}{\partial P_{n,t'}^{DG}} I_{ij,t'}^{Im} + V_{i,t'}^{Im}\frac{\partial I_{ij,t'}^{Im}}{\partial P_{n,t'}^{DG}} \tag{44}$$

Furthermore, $\partial J_{C_m}/\partial \boldsymbol{a_n}$ for the global constraints (3) and (4) can be calculated using the outcomes of Steps 2 and 3:

$$\frac{\partial V_{i,t'}}{\partial \boldsymbol{a_{n,t'}}} = \frac{V_{i,t'}^{Re}}{V_{i,t'}}\frac{\partial V_{i,t'}^{Re}}{\partial \boldsymbol{a_{n,t'}}} + \frac{V_{i,t'}^{Im}}{V_{i,t'}}\frac{\partial V_{i,t'}^{Im}}{\partial \boldsymbol{a_{n,t'}}} \tag{45}$$

$$\frac{\partial I_{ij,t'}}{\partial \boldsymbol{a_{n,t'}}} = \frac{I_{ij,t'}^{Re}}{I_{ij,t'}}\frac{\partial I_{ij,t'}^{Re}}{\partial \boldsymbol{a_{n,t'}}} + \frac{I_{ij,t'}^{Im}}{I_{ij,t'}}\frac{\partial I_{ij,t'}^{Im}}{\partial \boldsymbol{a_{n,t'}}} \tag{46}$$

2) $\partial \boldsymbol{a_n}/\partial \pi_n$: Using the latest values for parameters $\boldsymbol{\mu_n}$, Σ_n, and actions $\boldsymbol{a_n}$, the gradient of control actions w.r.t. π_n is obtained from (22), as follows [19]:

$$\frac{\partial \boldsymbol{a_n}}{\partial \pi_n} = -(\frac{\Sigma_n^{-1}(\boldsymbol{a_n} - \boldsymbol{\mu_n})}{\sqrt{|\Sigma_n|(2\pi)^{D_n}}}e^{-\frac{1}{2}A})^{-1} \tag{47}$$

where, $A = (\boldsymbol{a_n} - \boldsymbol{\mu_n})^\top \Sigma_n^{-1}(\boldsymbol{a_n} - \boldsymbol{\mu_n})$.

3) $\partial \pi_n/\partial \boldsymbol{\mu_n}$ and $\partial \pi_n/\partial \Sigma_n$: using the latest values for parameters $\boldsymbol{\mu_n}$, Σ_n and actions $\boldsymbol{a_n}$, the gradients of control policies, w.r.t. $\boldsymbol{\mu_n}$ and Σ_n are determined using (22):

$$\frac{\partial \pi_n}{\partial \boldsymbol{\mu_n}} = \frac{\Sigma_n^{-1}(\boldsymbol{a_n} - \boldsymbol{\mu_n})}{\sqrt{|\Sigma_n|(2\pi)^{D_n}}}e^{-\frac{1}{2}A} \tag{48}$$

$$\frac{\partial \pi_n}{\partial \Sigma_n} = -\frac{1}{2}\frac{(\Sigma_n^{-1} - \Sigma_n^{-1}(\boldsymbol{a_n} - \boldsymbol{\mu_n})(\boldsymbol{a_n} - \boldsymbol{\mu_n})^\top \Sigma_n^{-1})}{\sqrt{|\Sigma_n|(2\pi)^{D_n}}}e^{-\frac{1}{2}A} \tag{49}$$

4) $\partial \boldsymbol{\mu_n}/\partial \boldsymbol{\theta_{\mu_n}}$ and $\partial \Sigma_n/\partial \boldsymbol{\theta_{\Sigma_n}}$: A *back-propagation process* [20] is performed on the two DNNs within each MG agent's control policy function, (20) and (21), to determine the gradients of DNNs' outputs w.r.t. their parameters. In each iteration, the latest values of state variables are employed as inputs of the DNNs. The back-propagation process exploits chain rule for stage-by-stage spreading of gradient information through layers of the DNNs, starting from the output layer and moving towards the input [20]. To enhance the stability of the back-propagation process, a sample batch approach is adopted, where the gradients obtained from several sampled actions are averaged to ensure robustness against outliers.

IV. Multi-Agent Consensus-based Safe Policy Learning

Using the gradient factors (27) and (28), the QCLP, (23)-(25), is fully specified and can be solved at each policy update iteration for training the agents' PL frameworks. However, we have identified two challenges in this problem: (i) the size of the DNN parameters $\boldsymbol{\theta}$ can be extremely large, which results in high computational costs during training. (ii) The control policy privacy of the MG agents needs to be preserved during training, which implies that the agents might not have access to each others' control policy parameters. Centralized solvers can be both time-consuming and lack guarantees for privacy maintenance.

In order to address these two challenges, we have developed a *multi-agent consensus-based constrained training algorithm* [16]. Due to its distributed nature this method is both scalable and does not require sharing control policy parameters among agents. Thus, the proposed algorithm is able to efficiently solve the QCLP (23)-(25), while relying only on local inter-MG communication. The purpose of inter-MG interactions is to satisfy global constraints, (3)-(4). To do this, the agents repeatedly estimate and communicate dual variable $\boldsymbol{\lambda_n}$, corresponding to the Lagrangian multiplier of global constraints. Furthermore, a local primal-dual gradient step is included in the algorithm to move the primal and dual parameters towards their global optimum. The proposed distributed algorithm consists of four stages that are performed iteratively, as follows:

Stage I. *Initialize ($k \leftarrow 1$):* Gradient factors $\boldsymbol{g_n}$ and $\boldsymbol{b_m}$ are obtained from Section II-D. The previous values of learning parameters are input to the QCLP, $\boldsymbol{\theta_n^t}(0) \leftarrow \boldsymbol{\theta_n^{t-1}}$. Lagrangian multipliers are initialized as zero for each MG agent.

Stage II. *Weighted averaging operation:* MG agent n receives the Lagrangian multiplier $\boldsymbol{\lambda_{n'}}$, for global constraints

(3)-(4), from its neighbouring MG agents $n' \in \{1, ..., N_n\}$ and combines the received estimates using weighted averaging:

$$\bar{\boldsymbol{\lambda}}_{\boldsymbol{n}}(k) = \sum_{n'=1}^{N_n} w_n(n') \boldsymbol{\lambda}_{\boldsymbol{n'}}(k) \tag{50}$$

where, $w_n(n')$ is the weight that MG agent n assigns to the incoming message of the neighbouring MG agent, n'. To guarantee convergence to consensus, the weight matrix, composed of the agents' weight parameters $w_n(n')$, is selected as a doubly stochastic matrix [16].

Stage III. *Primal gradient update:* The n'th MG agent updates its primal parameters $\boldsymbol{\theta}_{\boldsymbol{n}}^{\boldsymbol{t}}$ employing a gradient descent operation, using the gradients of the agent's reward and the global constraint returns, $m' \in M^G$, and step size ρ_1:

$$\bar{\boldsymbol{\theta}}_{\boldsymbol{n}}(k) = \boldsymbol{\theta}_{\boldsymbol{n}}^{\boldsymbol{t}}(k) - \rho_1(\boldsymbol{g}_{\boldsymbol{n}}(\boldsymbol{\theta}_{\boldsymbol{n}}^{\boldsymbol{t}}(k)) + \boldsymbol{b}_{\boldsymbol{m'}}(\boldsymbol{\theta}_{\boldsymbol{n}}^{\boldsymbol{t}}(k))\bar{\boldsymbol{\lambda}}_{\boldsymbol{n}}(k)) \tag{51}$$

Stage IV. *Projection on local constraints:* The agent projects the local learning parameters to the feasible region defined by the gradients of the local constraints (5)-(14):

$$\boldsymbol{\theta}_{\boldsymbol{n}}^{\boldsymbol{t}}(k+1) = \arg\min_{\boldsymbol{\theta}} ||\bar{\boldsymbol{\theta}}_{\boldsymbol{n}}(k) - \boldsymbol{\theta}|| \tag{52}$$

$$s.t. \quad J_{c_m}(\boldsymbol{\theta}_{\boldsymbol{n}}^{\boldsymbol{t}}(0)) + \boldsymbol{b_m}^T(\boldsymbol{\theta}_{\boldsymbol{n}}^{\boldsymbol{t}}(0) - \boldsymbol{\theta}) \leq d_m, \ \forall m \in M^L \tag{53}$$

$$\frac{1}{2}(\boldsymbol{\theta}_{\boldsymbol{n}}^{\boldsymbol{t}}(0) - \boldsymbol{\theta})^T H_n(\boldsymbol{\theta}_{\boldsymbol{n}}^{\boldsymbol{t}}(0) - \boldsymbol{\theta}) \leq \delta, \ \forall n \tag{54}$$

Stage V. *Dual gradient update:* Each agent's estimations of dual variables $\boldsymbol{\lambda}_{\boldsymbol{n}}$ for the global constraints, (3) and (4), will be updated using a gradient ascent process over $\bar{\boldsymbol{\lambda}}_{\boldsymbol{n}}$:

$$\boldsymbol{\lambda}_{\boldsymbol{n}}(k+1) = [(\bar{\boldsymbol{\lambda}}_{\boldsymbol{n}}(k) + \rho_2(\boldsymbol{b_{m'}}\boldsymbol{\theta}_{\boldsymbol{n}}^{\boldsymbol{t}}(k+1) - d_{m'})]^+, \forall m' \in M^G \tag{55}$$

where, ρ_2 is a penalty factor for global constraints violation, and the operator $[\cdot]^+$ returns the non-negative part of its input.

Stage VI. *Stopping criteria:* Check algorithm convergence using the changes of $\boldsymbol{\theta}_{\boldsymbol{n}}^{\boldsymbol{t}}(k)$; stop when the changes in parameters falls below the threshold value $\Delta\theta_n$; otherwise, go back to Stage II.

The overall flowchart of the multi-agent safe PL process using the proposed distributed training technique is shown in Algorithm 1.

Algorithm 1 Multi-agent Safe Policy Learning

Select T, ρ_1, ρ_2
Initialize $\boldsymbol{\theta}_{\boldsymbol{n}}^{\boldsymbol{t_0}}$
for $t \leftarrow 1$ to t^{max} **do**
  $\boldsymbol{S_n} \leftarrow [\boldsymbol{S_n}(t), ..., \boldsymbol{S_n}(t+T)]$
  $\boldsymbol{\mu_n} \leftarrow$ (20) [Parameter insertion]
  $\boldsymbol{\Sigma_n} \leftarrow$ (21) [Parameter insertion]
  $\boldsymbol{a_n} \sim \pi_n(\boldsymbol{S_n}|\boldsymbol{\theta_n}) \leftarrow$ (22) [Action selection]
  $\partial J_{R_n}/\partial \boldsymbol{a_n} \leftarrow$ (43)-(44)
  $\partial J_{C_m}/\partial \boldsymbol{a_n} \leftarrow$ (29), (45)-(46)
  $\partial \boldsymbol{a_n}/\partial \pi_n \leftarrow$ (47)
  $\partial \pi_n/\partial \boldsymbol{\mu_n} \leftarrow$ (48)
  $\partial \pi_n/\partial \Sigma_n \leftarrow$ (49)
  $\partial \boldsymbol{\mu_n}/\partial \boldsymbol{\theta_{\mu_n}} \leftarrow DNN_{\mu_n}$ [Back-propagation]
  $\partial \Sigma_n/\partial \boldsymbol{\theta_{\Sigma_n}} \leftarrow DNN_{\Sigma_n}$ [Back-propagation]
  $\boldsymbol{g_{\mu_n}}, \boldsymbol{b_{m,\mu_n}} \leftarrow$ (27) [Chain rule]
  $\boldsymbol{g_{\Sigma_n}}, \boldsymbol{b_{m,\Sigma_n}} \leftarrow$ (28) [Chain rule]
  $H_n \leftarrow$ (26) [FIM Construction]
  Initialize $\boldsymbol{\lambda_n}(k_0)$
  for $k \leftarrow 1$ to k^{max} **do**
    $\bar{\boldsymbol{\lambda}}_{\boldsymbol{n}}(k) \leftarrow$ (50) [Averaging operation]
    $\bar{\boldsymbol{\theta}}_{\boldsymbol{n}}(k) \leftarrow$ (51) [Primal gradient update]
    $\boldsymbol{\theta}_{\boldsymbol{n}}^{\boldsymbol{t}}(k+1) \leftarrow$ (52)-(54) [Projection on M^L]
    $\boldsymbol{\lambda_n}(k+1) \leftarrow$ (55) [Dual gradient update]
    if $||\boldsymbol{\theta}_{\boldsymbol{n}}^{\boldsymbol{t}}(k+1) - \boldsymbol{\theta}_{\boldsymbol{n}}^{\boldsymbol{t}}(k)|| \leq \Delta\theta_n$ **then**
      $\boldsymbol{\theta}_{\boldsymbol{n}}^{\boldsymbol{t+1}} \leftarrow \boldsymbol{\theta}_{\boldsymbol{n}}^{\boldsymbol{t}}(k+1)$; Break;
    end if
  end for
  if $||\boldsymbol{\theta}_{\boldsymbol{n}}^{\boldsymbol{t+1}} - \boldsymbol{\theta}_{\boldsymbol{n}}^{\boldsymbol{t}}|| \leq \Delta\theta_n$ **then**
    Output $\boldsymbol{\theta}_{\boldsymbol{n}}^{\boldsymbol{t+1}}$; Break;
  end if
end for

V. Simulation Results

The proposed method is tested on a modified 33-bus distribution network [21], which consists of five MGs as shown in Fig. 2a. Each MG is modeled as a modified IEEE 13-bus network [21] at a low voltage level as shown in Fig. 2b.

In this case study, the energy price for the transferred power at the MG PCCs and the fuel price for the local DGs are adopted from [22] and [23], respectively. The input data load demands and PV generations data with 15 minutes time resolution are both obtained from smart meters to provide realistic numerical experiments [24]. All the case studies are simulated using a PC with Intel Core i7-4790 3.6 GHz CPU and 16 GB RAM hardware. The simulations are performed in MATLAB, OpenDSS, and GAMS to obtain the gradient factors, update the learning parameters, solve the distributed training problem, and validate the results.

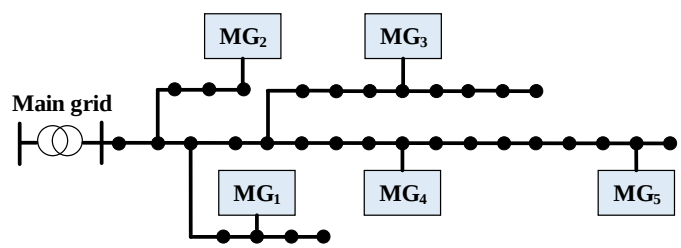

(a) 33-bus system for distribution network

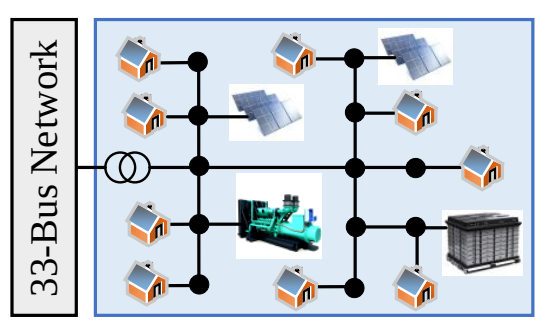

(b) 13-bus system for MGs

Fig. 2. Test system under study.

A. System Operation Outcomes

The aggregate MG demand, aggregate MG generation, and aggregate power transfer through PCCs of MGs over a day are shown in Fig. 3. It can be seen that the main MG demands are supplied by the local generation within MGs due to low DG fuel prices and renewable outputs. While most MGs are exporting power to the upstream distribution grid, MG_4 is importing power to satisfy the heavy local load that cannot be fully supplied internally. In all cases the power balance is maintained within the MGs. The ESS charging/discharging power outputs and SOCs for each MG are shown in Fig. 4, where as can be seen the ESSs charge during off-peak period and discharge during peak time to provide optimal power balancing support for MGs.

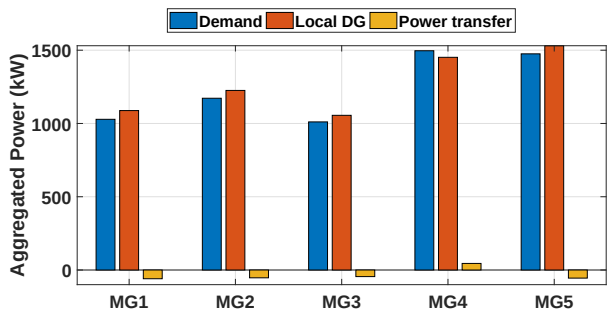

Fig. 3. Aggregated power of local demand, local DG generation and power transfer for MG_1-MG_5.

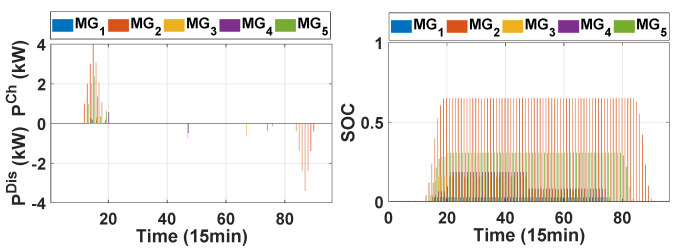

(a) ESS charging/discharging powers (b) ESS SOCs

Fig. 4. ESS dispatching results for MG_1-MG_5.

Table II presents a comparison between a conventional commercial centralized optimization solver and the proposed safe PL in terms of MGs' operational costs in one decision window. It can be seen that the MGs' operational costs from both methods are relatively close to each other, since both the centralized optimization method and the proposed safe PL search for the optimal solutions to maximize the social welfare. However, compared to centralized optimization our method provides instantaneous response to time-varying system conditions after completing the training process, instead of solving a new complex optimization problem at each time step. Even though the PL training process takes time, the decision time for the proposed safe PL is only 7.46 seconds, which is much shorter than 65.45 seconds for the centralized optimization solver. Furthermore, due to its distributed nature, the proposed PL technique maintains MG privacy.

B. Algorithm Performance

Fig. 5a and Fig. 5b show the convergence of a select group of learning parameters, $\boldsymbol{\theta_\mu}$ and $\boldsymbol{\theta_\Sigma}$, for each MG agent. As can be seen, the changes in $\boldsymbol{\theta_\mu}$ are relatively larger than that of $\boldsymbol{\theta_\Sigma}$. This is due to the higher levels of sensitivity of MG agents' objective functions to the mean values of the control actions compared with their variance levels.

TABLE II
COMPARISON OF MGS' OPERATIONAL COSTS IN ONE DECISION WINDOW

	MG_1	MG_2	MG_3	MG_4	MG_5
Centralized opt. ($)	22.123	22.339	20.796	26.378	23.061
Safe PL ($)	21.679	21.827	21.571	27.002	23.919
Difference (%)	2.01	2.29	-3.73	-2.37	-3.59

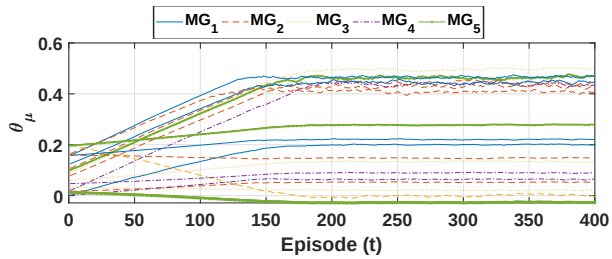

(a) Select θ_μ's during training process

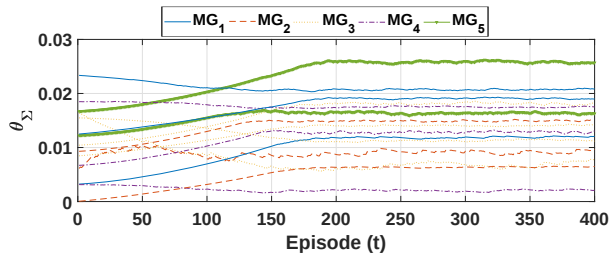

(b) Select θ_Σ's during training process

Fig. 5. Convergence of learning parameters θ_μ and θ_Σ for MG_1-MG_5 .

To better show the performance of the proposed safe PL method and the importance of considering constraints during the training process, we have compared three cases: (i) DG capacity constraints are in place for all MGs; (ii) no DG capacity constraints in MG_1 and MG_2; (iii) no DG capacity constraints in MG_1-MG_5. As can be seen in Fig. 6, in cases (ii) and (iii), the agents obtain a higher reward compared to case (i) due to the constraint omission; however, this comes at the expense of decision infeasibility. In case (i), these operational constraints are satisfied, which also leads to a drop in total reward, as expected. This shows that our proposed constrained PL decision model guarantees the feasibility of the control actions w.r.t. the constraints of the power management problem.

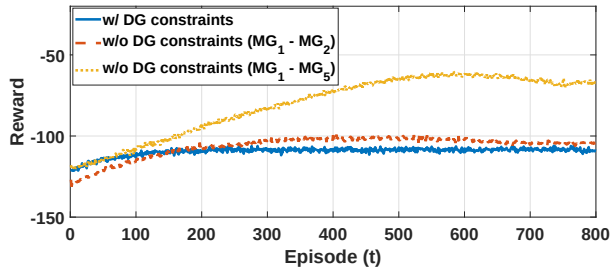

Fig. 6. Comparison of reward w/ and w/o DG capacity constraints of different MGs.

Furthermore, Fig. 7 shows the constraint return values at during the training iterations for a 1-hour time window, for the two cases with and without DG capacity constraints in MG_1, where each curve in the figure represents constraint return at one 15-minute time instant. As can be seen, the conventional unconstrained solver violates the upper boundary for the constraint return limit for all time instants; on the other hand, the proposed safe PL solver satisfies the DG generation capacity constraints, which implies that the constraint return values do not violate the DG capacity limits.

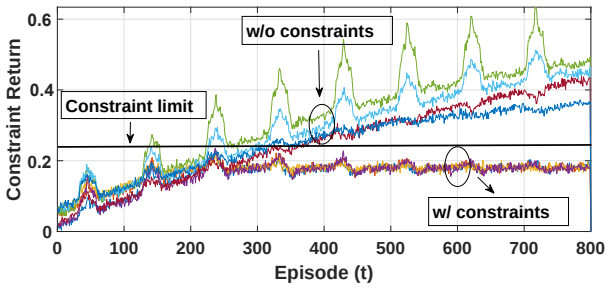

Fig. 7. Comparison of constraint return values for w/ and w/o the DG capacity constraints in MG_1.

One example of the distributed training convergence process is shown in Fig. 8 for a policy gradient update step. As can be seen, the Lagrangian multipliers λ_n reach zero over iterations of the proposed multi-agent algorithm, which indicates that all the global constraints, including nodal voltage and branch current limits, are satisfied and optimal feasible solutions are obtained.

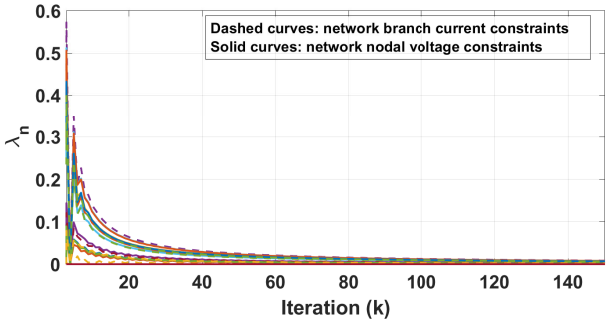

Fig. 8. The performance of the iterative distributed training method in one episode.

VI. Conclusion

Conventional model-based optimization methods suffer from high computational costs when solving large-scale multi-MG power management problems. On the other hand, the conventional model-free methods are black-box tools, which may fail to satisfy the operational constraints. Motivated by these challenges, in this paper, a multi-agent safe PL method has been proposed for power management of networked MGs. Our proposed method exploits the gradients of the decision problem to learn control policies that achieve both optimality and feasibility. Furthermore, to enhance computational efficiency and maintain the policy privacy of the control agents, a distributed consensus-based training process is implemented to update the agents' policy functions over time using local communication.

References

[1] Z. Li, M. Shahidehpour, F. Aminifar, A. Alabdulwahab, and Y. Al-Turki, "Networked microgrids for enhancing the power system resilience," *Proc. of the IEEE*, vol. 105, no. 7, pp. 1289–1310, July 2017.

[2] M. N. Alam, S. Chakrabarti, and A. Ghosh, "Networked microgrids: State-of-the-art and future prospectives," *IEEE Trans. Ind. Informat.*, vol. 15, pp. 1238–1250, March 2019.

[3] M. Ban, M. Shahidehpour, J. Yu, and Z. Li, "A cyber-physical energy management system for optimal sizing and operation of networked nanogrids with battery swapping stations," *IEEE Trans. Sustain. Energy*, vol. 10, no. 1, pp. 491–502, Jan 2019.

[4] Z. Wang, B. Chen, J. Wang, M. Begovic, and C. Chen, "Coordinated energy management of networked microgrids in distribution systems," *IEEE Trans. Smart Grid*, vol. 6, no. 1, pp. 45–53, Jan. 2015.

[5] Z. Wang, B. Chen, J. Wang, and J. Kim, "Decentralized energy management system for networked microgrids in grid-connected and islanded modes," *IEEE Trans. Smart Grid*, vol. 7, no. 2, pp. 1097–1105, March 2016.

[6] D. Shi, X. Chen, Z. Wang, X. Zhang, Z. Yu, X. Wang, and D. Bian, "A distributed cooperative control framework for synchronized reconnection of a multi-bus microgrid," *IEEE Trans. Smart Grid*, vol. 9, no. 6, pp. 6646–6655, Nov 2018.

[7] B. Zhao, X. Wang, D. Lin, M. M. Calvin, J. C. Morgan, R. Qin, and C. Wang, "Energy management of multiple microgrids based on a system of systems architecture," *IEEE Trans. Power Syst.*, vol. 33, no. 6, pp. 6410–6421, Nov 2018.

[8] J. Duan, Z. Yi, D. Shi, C. Lin, X. Lu, and Z. Wang, "Reinforcement-learning-based optimal control for hybrid energy storage systems in hybrid ac/dc microgrids," *IEEE Trans. Ind. Informat.*, vol. 15, no. 9, pp. 5355–5364, Sept 2019.

[9] P. Zeng, H. Li, H. He, and S. Li, "Dynamic energy management of a microgrid using approximate dynamic programming and deep recurrent neural network learning," *IEEE Trans. Smart Grid*, vol. 10, no. 4, pp. 4435–4445, 2019.

[10] B. Kim, Y. Zhang, M. van der Schaar, and J. Lee, "Dynamic pricing and energy consumption scheduling with reinforcement learning," *IEEE Trans. Smart Grid*, vol. 7, no. 5, pp. 2187–2198, Sept. 2016.

[11] T. Yu, H. Z. Wang, B. Zhou, K. W. Chan, and J. Tang, "Multi-agent correlated equilibrium Q learning for coordinated smart generation control of interconnected power grids," *IEEE Trans. Power Syst.*, vol. 30, no. 4, pp. 1669–1679, July 2015.

[12] Q. Zhang, K. Dehghanpour, Z. Wang, and Q. Huang, "A learning-based power management method for networked microgrids under incomplete information," *IEEE Trans. Smart Grid*, Early access.

[13] J. Achiam, D. Held, A. Tamar, and P. Abbeel, "Constrained policy optimization," *in Proc. of 34th International Conference on Machine Learning*, 2017.

[14] M. Wen and T. Ufuk, "Constrained cross-entropy method for safe reinforcement learning," *in Proc. of 32nd Conference on NeurIPS*, 2018.

[15] Y. Chow, O. Nachum, M. Ghavamzadeh, and E.Duen, "A lyapunov-based approach to safe reinforcement learning," *in Proc. of 32nd Conference on NeurIPS*, 2018.

[16] T. H. Chang, A. Nedic, and A. Scaglione, "Distributed constrained optimization by consensus-based primal-dual pertubation method," *IEEE Trans. Automatic Control*, vol. 59, no. 6, pp. 1524–1538, June 2014.

[17] O. Besson and Y. I. Abramovich, "On the fisher information matrix for multivariate elliptically contoured distributions," *IEEE Signal Processing Letters*, vol. 22, no. 11, pp. 1130–1133, Nov. 2013.

[18] R. A. Jabr and I. Dafi, "Sensitivity-based discrete coordinate-descent for volt/var control in distribution networks," *IEEE Trans. Power Syst.*, vol. 31, no. 6, pp. 4670–4678, Nov. 2016.

[19] P. K. Brandt and M. S. Pedersen, *The Matrix Cookbook*. Technical University of Denmark, 2008.

[20] J. Li, J. Cheng, J. Shi, and F. Huang, "Brief introduction of back propagation neural network algorithm and its improvement," *Advances in computer science and information engineering*, pp. 553–558, 2012.

[21] W. Kersting, "Radial distribution test feeder," *in Proc. of 2001 IEEE PES Winter Meeting*, vol. 2, pp. 908–912, 2001.

[22] Wholesale electricity and natural gas market data. [Online]. Available: https://www.eia.gov/electricity/wholesale/#history

[23] Gasoline and diesel fuel update. [Online]. Available: https://www.eia.gov/petroleum/gasdiesel/

[24] Iowa distribution test systems. [Online]. Available: http://wzy.ece.iastate.edu/Testsystem.html